U.S. Department
of Transportation

**Federal Railroad
Administration**

Stress Reconstruction Analysis of Wheel Saw Cut Tests and Evaluation of Reconstruction Procedure

Office of Research
and Development
Washington, DC 20590

Y. H. Tang
J. E. Gordon
O. Orringer
A. B. Perlman

Research and
Special Programs
Administration
John A. Volpe National
Transportation Systems Center
Cambridge, MA 02142-1093

DOT/FRA/ORD-93/18
DOT-VNTSC-FRA-93-22

Final Report
September 1993

NOTICE

This document is disseminated under the sponsorship of the Department of Transportation in the interest of information exchange. The United States Government assumes no liability for its contents or use thereof.

NOTICE

The United States Government does not endorse products or manufacturers. Trade or manufacturers' names appear herein solely because they are considered essential to the object of this report.

REPORT DOCUMENTATION PAGE

Form Approved
OMB No. 0704-0188

1. AGENCY USE ONLY (Leave blank)	2. REPORT DATE	3. REPORT TYPE AND DATES COVERED
	September 1993	Final Report December 1992 - March 1993

4. TITLE AND SUBTITLE
Stress Reconstruction Analysis of Wheel Saw Cut Tests and Evaluation of Reconstruction Procedure

5. FUNDING NUMBERS
R3026/RR328

6. AUTHOR(S)
Y.H. Tang, J.E. Gordon, O. Orringer and A.B. Perlman

7. PERFORMING ORGANIZATION NAME(S) AND ADDRESS(ES)
U.S. Department of Transportation
Research and Special Programs Administration
John A. Volpe National Transportation Systems Center
Cambridge, MA 02142

8. PERFORMING ORGANIZATION REPORT NUMBER
DOT-VNTSC-FRA-93-22

9. SPONSORING/MONITORING AGENCY NAME(S) AND ADDRESS(ES)
Federal Railroad Administration
Office of Research and Development
Washington, DC 20590

10. SPONSORING/MONITORING AGENCY REPORT NUMBER
DOT/FRA/ORD-93/18

11. SUPPLEMENTARY NOTES

12a. DISTRIBUTION/AVAILABILITY STATEMENT
This document is available to the public through the National Technical Information Service, Springfield, VA 22161

12b. DISTRIBUTION CODE

13. ABSTRACT (Maximum 200 words)

This report is the fourth in a series of engineering studies on railroad vehicle wheel performance. The results of saw cut tests performed on one new and one used wheel designed for a fleet of multiple unit (MU) power cars are summarized and analyzed. Reconstructed residual stresses are computed in the usual manner, namely: by modeling the deformed cut wheel with finite elements and prescribing displacements to close the cut. Similar cases are computed, with thermal stresses calculated from a companion finite element model to play the role of residual stresses, in order to simulate the experiment reconstruction analysis. Comparison with the exact thermal stresses show that the conventional reconstruction procedure is not accurate, even when the cut opening profile data has been supplemented by measurements of radial displacement along the cut, relative to the cut tip. Better results are obtained from the simulation of an experiment with measurements of absolute radial displacement. Several possible refinements of the saw cut test measurement procedures are suggested.

14. SUBJECT TERMS
Residual Stress; Saw Cut Tests; Wheels

15. NUMBER OF PAGES
38

16. PRICE CODE

17. SECURITY CLASSIFICATION OF REPORT	18. SECURITY CLASSIFICATION OF THIS PAGE	19. SECURITY CLASSIFICATION OF ABSTRACT	20. LIMITATION OF ABSTRACT
Unclassified	Unclassified	Unclassified	

PREFACE

This report is the fourth of a series of engineering studies on railroad vehicle wheel performance. The first report summarized an evaluation of actions taken to respond to high rates of crack occurrence observed in the wheels of certain multiple unit (MU) power cars used in commuter service. The second and third reports dealt with experimental and analytical evaluations of heating effects, caused by friction braking on the wheel treads, when the wheels are subjected to typical commuter service stops.

In this report, the results of earlier saw cut tests are summarized, and the data is analyzed to reconstruct the residual stresses which existed in each of two wheels before cutting. The reconstruction procedure was also simulated to evaluate the accuracy of such experiments, and the results demonstrated the need for better measurements, if the objective is to determine the residual stress distribution. More extensive measurements are planned for the next saw cut tests, which will be documented in a later report in this series.

The purposes of such measurements are to characterize initial (as-manufactured) conditions, as well as to sample the residual stress states in wheels which have been subjected to friction braking during service. Descriptions of initial stress states are required as input to models used for prediction of residual stresses in service. Measurements of service stresses are required for validation of the predictive models.

LIST OF ILLUSTRATIONS

LIST OF ILLUSTRATIONS (Cont'd)

LIST OF TABLES

1. INTRODUCTION

This report is the fourth of a series on the results of an engineering study of the effects of service loads on railroad vehicle wheels. The study was initiated in September 1991, in response to a request for assessment of contributing factors and corrective actions taken regarding high rates of crack occurrence in certain multiple unit (MU) powered cars used in commuter service. The ultimate goal of the study is the evaluation of safe limits on performance demand (weight carried per wheel, maximum speed, vehicle braking rate) as a function of wheel design, material selection, and manufacture, as well as percentage of braking effort absorbed through the wheel tread in service. The models developed in the study are intended to provide the capability for similar engineering design analyses of other railroad vehicle wheels besides the types used on MU cars.

1.1 Background

Special inspections of commuter rail vehicles conducted by the Federal Railroad Administration (FRA) Office of Safety in 1991 revealed chronic problems of cracking in the wheels of powered MU cars operated by three railroads serving the Greater New York area. The car design types are similar, but the vehicle characteristics and wheel cracking features were found to have significant differences.

The highest rate of cracking was found in the wheels of moderate weight vehicles, operated at moderate speeds, and equipped with blended dynamic braking to supplement the wheel tread brakes. The wheel cracks in this fleet, predominantly of thermal origin at the front rim edge, were attributed to maintenance problems: (1) dispatching of vehicles with inoperative traction motors, and thus also inoperative dynamic braking; and (2) inadequate tread brake unit refurbishment, leading to brake shoes riding over the front rim edge.

A comparable rate of cracking was found in the wheels of moderate weight vehicles, operated at high speed (100 mph), and equipped solely with tread brakes. The wheel cracks in this fleet, of thermal origin in the center tread position, were attributed to the demand for heat absorption through the tread imposed by high-speed operation without auxiliary brakes.

A lower rate of cracking with mixed thermal and mechanical origins was found in the third fleet. This fleet consists of heavy vehicles, operated at moderate speeds, and equipped with blended dynamic braking to supplement the tread brakes. The combination of vehicle weight, heat input to the wheel tread, and occasional maintenance problems were identified as the factors contributing to wheel cracks in this case.

The FRA Office of Safety took immediate actions to assure continuing operational safety as soon as evidence of chronic wheel cracking was revealed. These actions included specific requirements to address identified maintenance problems and general requirements for daily inspection of wheels in service. Wheels found to have cracks must be shopped and re-trued to remove all crack indications before return to service. The general requirements prudently established a safety first policy, under the circumstances of frequent crack occurrence but lack of accurate critical[1] crack size information. Since compliance places economic burdens on

---

1 "Critical" as used here means a crack just large enough to precipitate wheel fracture under existing service conditions.

the affected railroads, the Office of Safety requested an engineering study to: (1) evaluate the effectiveness of the immediate actions; and (2) develop rational options for long-term solutions.

Each affected railroad also started to take longer term actions and develop options for lasting solutions. Actions already taken include upgrade of material properties and adoption of an advanced plate design in the specifications for new wheel orders and, for those MU cars not so equipped, retrofit of new motors with dynamic braking capability. Options under development include route studies to identify segments where speed reductions might provide effective relief without undue schedule penalty, further advancement of wheel design, and improvement of brake shoe material and/or design.

1.2 Preliminary Engineering Studies

Several preliminary study tasks were undertaken from September 1991 through September 1992. Initially, the wheel maintenance records of the affected railroads were reviewed to confirm the general nature of the crack occurrence patterns.[2] The frequency of re-trueing in some cases suggested that wheels were developing visible thermal cracks in weeks. Wheel service life in such cases appeared to be limited by the re-trueing necessary to remove crack indications.

Two wheels removed from service for center tread thermal cracks were destructively tested to obtain quantitative data on the number and size of the cracks [1]. Each tread surface was first surveyed with the aid of fluorescent magnetic particle inspection to locate the cracks and measure their visible lengths. Each wheel was then mounted on a vertical boring mill and re-faced in short steps from the front rim face toward the flange to permit determination of the crack depths.[3] The test wheels were found to have, respectively, 69 and 160 identifiable center tread thermal cracks with visible lengths ranging from 0.5 inch (13 mm)[4] to 1.15 inches (29 mm), with no crack depth exceeding 0.33 inch (8.4 mm). The other significant findings were that all cracks were visible on the tread surface, and that the visible length of each crack was also its maximum length.

A new wheel and the mate to one of the above wheels were also subjected to destructive saw cutting to provide displacement data for estimation of residual stresses in the rim.[5] The procedure for measuring the displaced cut profile was improved by means of moire instrumentation [2], but the method used to estimate the residual stresses from the displacement data was the same as that developed by the Association of American Railroads (AAR) for an earlier program of research on freight car wheels [3]. The analysis of test results indicated outer rim hoop stresses about 42 ksi (290 MPa) compression in the new wheel but

---

2 Inquiries were also made through other FRA region offices to determine whether other railroads were experiencing similar problems (no comparable occurrence rates were found).

3 Shop support was provided by the ORX Railway Corporation, Tipton, PA.

4 Center tread thermal cracks do not become visually identifiable as such until the visible length reaches about 1/2 inch.

5 Shop support was provided by the Norfolk Southern Railroad Research Laboratory, Alexandria, VA.

only 20 ksi (140 MPa) compression in the used wheel. The retention of some compression in a used wheel was encouraging, since compressive stress tends to close and delay the growth of cracks. However, the saw cut tests did not provide the data necessary to reliably determine the depth below tread at which a crack would encounter tensile hoop stress.

Metallographic examination and hardness testing [4] of sections taken from the mate wheel established depth below tread limits for the following phenomena: (1) heavily deformed plastic zone indicated by sheared elongated grain shape to a depth of 0.0008 inch (0.02 mm); (2) heat affected zone indicated by presence of spherodized microstructure to a depth of 0.02 inch (0.5 mm); and (3) layer work-hardened to an approximate average of RC 43 to a depth of 0.02 inch (0.5 mm).[6] Fractographic examination of fatigue crack growth surfaces confirmed the tendency of the cracks to grow much more slowly in depth as the maximum depth approached 0.2 to 0.3 inch (5 to 8 mm), but lateral growth toward the flange and front rim face appeared to continue unabated. Conversely, fractographic examination of another center tread crack in a wheel that had also been subjected to drag-braking showed evidence of rapid propagation (fracture and arrest) events, beginning when the crack was about 1/2 inch long on the tread surface.

Laboratory specimens from the new wheel were also subjected to combined high temperature and rapid plastic compression, followed by air cooling, to simulate the combination of stop-braking and wheel/rail contact effects [5]. Metallographic examination [6] revealed a spherodized microstructure, similar to that observed near the used wheel tread, in those specimens which had been subjected to at least 5% compressive strain and temperatures in the pearlite - austenite transformation range, 1340 to 1430 ^{o}F (727 to 777 ^{o}C).

Heat transfer calculations with a preliminary model also suggested that wheel tread temperatures up to 1300 ^{o}F (704 ^{o}C) could be attained as a result of the high-performance stop-braking profiles experienced by the MU cars. More detailed calculations with a finite element model showed that an overhanging brake shoe could produce temperatures in the transformation range near the front rim edge, under otherwise normal operating conditions.

The picture which emerged from the preliminary studies suggested that cracks of thermal origin are the main concern, and that a process of shallow stress reversal is responsible for the formation of such cracks in the wheels of the MU cars. Stress reversal (from hoop compression to tension) is a well known cause of thermal cracking and fracture in freight car wheels which have been subjected to repeated drag braking for long period of time at low power, but in such cases the stress is usually reversed in the bulk of the rim, most of which is heated to high temperature. Conversely, typical stop-braking profiles involve high power for short period of time and tend to flash-heat the outer rim region to temperatures much higher than those in the bulk of the rim. The thermal stresses, which are induced by temperature gradients, then concentrate in the outer rim region. Thus, wheel thermal response to stop-braking is not necessarily indicated by its response to drag-braking. Also, any subsequent drag-braking can apparently cause rapid propagation of thermal cracks which have formed under less severe conditions.

---

6 The base material has a pearlitic microstructure with approximate hardness RC 35 below the heat-affected and work-hardened zones.

Based on these findings, the decision was made to develop a set of detailed finite element models which could be used to evaluate the potential for different types of wheels to resist cracking under various combinations of service conditions. The approach, relation between models, and relation of models to validation tests are outlined in the following section.

1.3 Overview of Detailed Engineering Studies

The wheels of a typical MU car experience on the order of 10^4 stop-braking events and 10^7 wheel/rail contact cycles[7] in a year of service. Many stops and contact cycles are thus involved, even if rim stress is reversed in just a few days or weeks. The performance demand (weight carried per wheel, maximum speed, vehicle braking rate) may either modify or reverse the residual hoop stress in the rim. These outcomes can be distinguished by assuming that the modified or reversed stresses are stable, i.e., they are not changed simply by further repetition of the same performance demands after some period of service has elapsed. Such states, referred to as shakedown stresses, can be calculated from the known initial conditions (residual stress from manufacture) and descriptions of the loads imposed by repeated performance demands.

A recently developed method for estimating shakedown stresses in a body requires only that each load be described in terms of the stress magnitudes it would cause in the body, assuming purely elastic behavior [7]. This task is easily accomplished by means of elastic finite element stress analysis models. The method has been successfully applied to the problem of estimating shakedown stresses in rails [8], including cases in which initial conditions must be accounted for [9,10]. This method can also be used to estimate wheel shakedown stresses, with both mechanical (weight per wheel) and thermal (braking) loads as inputs.

The block diagram in Figure 1 illustrates the organization of models and tests required to develop a realistic procedure for estimating wheel shakedown stresses. The shaded blocks denote items covered in this report. The dashed box encloses those items which constitute the inputs and output of the wheel shakedown stress model.

The other blocks in Figure 1 represent the tasks required to prepare the inputs for the shakedown stress model. The theoretical paths are emphasized because the models can produce complete descriptions of input stresses which also conform to the laws of mechanical equilibrium. Completeness and conformity are necessary to avoid propagation and amplification of numerical errors in the shakedown stress calculations. Conversely, experimental stress analyses usually cover only part of the body, and the results often contain equilibrium errors when measurements are made on complex bodies such as wheels or rails [3,8]. In spite of these limitations, experiments are still essential for checking the realism of the models.

Two-dimensional heat transfer and elastic-plastic stress finite element models can be used to estimate the manufacturing stresses, under the reasonable assumption that the heat treatment process is axially symmetric. The heat and stress analyses are done independently,

---

7 "Cycle" refers to the repetition of contact stresses, at a typical point in the rim, in each wheel revolution.

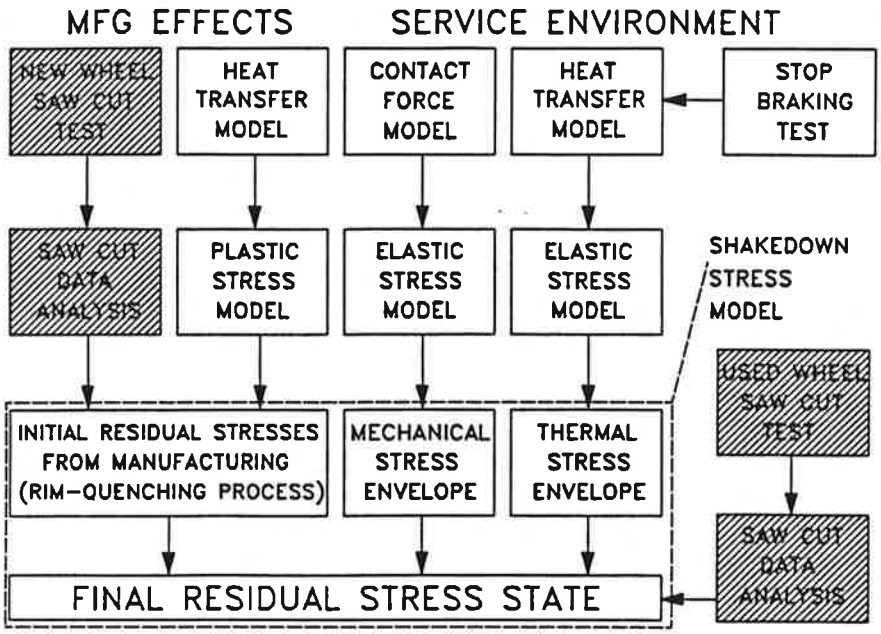

Figure 1. Model and Test Relationships.

but each requires further assumptions about physical parameters and high-temperature material properties. The model parameters must be adjusted until the calculated outer rim hoop stress is in reasonable agreement with the saw cut data analysis results.

Wheel/rail contact is generally modeled by means of semi-analytical techniques based on influence functions. The influence function is a description of displacements or stresses, in either body, caused by a concentrated force of unit magnitude applied to the body's surface. The theory of contact mechanics is mainly concerned with the application of displacement influence functions to calculate the area of contact, together with distributions of pressure and shear on the contact area, under various assumptions about the behavior of the contacting bodies [11]. For engineering design or detailed stress analysis, the contact model is often simplified by treating the bodies as elastic media and applying the basic Hertz contact theory. Calculations of this type have been used to provide the imposed stress input to incremental elastic-plastic finite element analyses of wheels [12,13]. A similar approach is taken in the present case, but with the added advantage that the elastic contact analysis is consistent with the assumptions of the shakedown theory. The numerical analysis must be three-dimensional, however, including a three-dimensional finite element model to account for the gross load stresses, even though the shakedown analysis itself is ultimately two-dimensional in character.

Thermal stress analysis requires only a two-dimensional finite model, under the reasonable assumption that the wheel revolves rapidly enough to distribute the braking energy axisymmetrically. Elastic material behavior may be assumed, in accordance with the shakedown model input requirements. The essential validation requirement is comparison

of temperature distributions calculated from the corresponding axisymmetric heat transfer model with temperature data measured near the wheel tread, under the transient conditions of stop-braking.

The most challenging tasks are those required for estimation of initial manufacturing stresses. The saw cut test and data analysis provide only a partial indication of the residual stresses in a wheel. Accurate information can be obtained about the distribution of hoop stress in the outer rim, where the cut has passed through, because the hoop component is fully relieved at the cut surface. The other stress components are only partially relieved at the cut, and only minor relief occurs at locations beyond the cut. However, the measured outer rim hoop stress provides a good check on the order of magnitude of the residual stresses calculated from the models.

One more opportunity to compare the model predictions with experimental results is provided by a saw cut test and displacement data analysis of a used wheel which shows evidence of thermal crack formation. As mentioned earlier, the data from such a test can at most provide an order-of-magnitude comparison for outer rim hoop stress, and in the present case even that comparison might be distorted if the cracks themselves are large enough to have relieved a significant amount of the hoop stress.

The saw cutting tests conducted as part of the preliminary studies [2] (Section 1.2) also served as a first attempt to obtain data of sufficient quality for the validation tasks depicted in Figure 1. Those experiments are re-examined in this report (Section 2), and the details of the reconstruction analysis are presented (Section 3). The reconstruction analysis procedure itself is also reconsidered, and some of its limitations are demonstrated by means of numerical simulation (Section 4).

2. SAW CUT TEST PROCEDURE AND RESULTS

The wheel saw cutting test is a practical expression of a fundamental concept in the mechanics of solid bodies containing residual stress. Where the cut creates new free surfaces, some stresses are relieved, and the relief is accompanied by deformations. If a wheel is cut radially, the major relief occurs in the hoop stress component, and the major associated deformation is circumferential. Thus, the kerf tends to open or close, depending upon whether hoop tension or compression is being relieved (Figure 2).

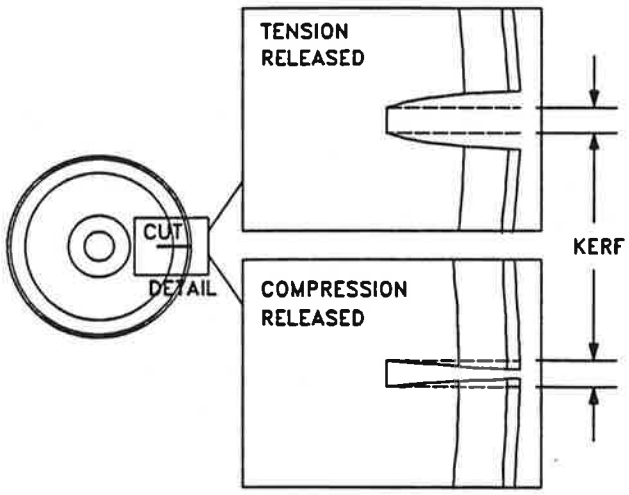

Figure 2. Saw Cut Test Concept.

2.1 Established Procedures

The Norfolk Southern Railroad pioneered the development of the following quantitative procedure. A small steel bar is first bonded or welded to the flange, astride the path of the cut, as shown in Figure 3(a). The cut is then started, and a clip-gauge extensometer is mounted across the severed bar when the saw blade is contained within the kerf, as shown in Figure 3(b). As the cut continues, the extensometer measures the relative circumferential displacement between the bar pieces, and this measurement can be interpreted for practical purposes as the opening or closing of the flange tip. Recording the extensometer reading on an XY plotter together with a linear voltage differential transformer (LVDT) measurement of the saw blade travel then produces a so-called clip-gauge curve. The character of the clip-gauge curve, Figure 3(c), indicates the condition of the uncut wheel.

The AAR developed a reconstruction analysis method, based on a representation of the wheel as a set of concentric rings [14], and applied the quantitative method to a comprehensive survey of freight car wheel conditions [15]. The analysis provides a rough estimate of the average hoop stress in the rim and is useful for evaluating the risk of fracture from a rim crack in a wheel of similar condition.

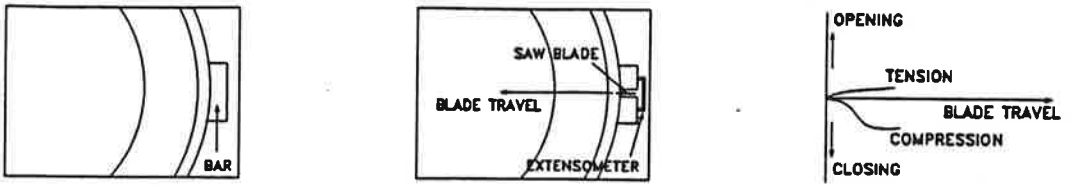

(a) preparation (b) instrumentation (c) clip-gauge curves

Figure 3. Quantitative Saw Cut Test.

The procedure was concurrently refined by the addition of cut profile measurements and use of a three-dimensional finite element model to perform the stress reconstruction. The refined procedure was applied to a small number of wheels after the cut had been extended into the plate in each case [3]. The relative displacement was measured with a steel ruler at intervals of approximately 10 mm on the front and back faces. The raw data was corrected by subtracting an estimate for the kerf, based on the saw blade thickness (Figure 4). Half- and quarter-symmetric models were tried, and the quarter-symmetric model was adopted when no significant difference was found between the two sets of computed stresses. In either case, the cut profile is represented in the initial geometry of the model (Figure 5), and the stresses are reconstructed by imposing counter displacements to return the cut surface to the center line.

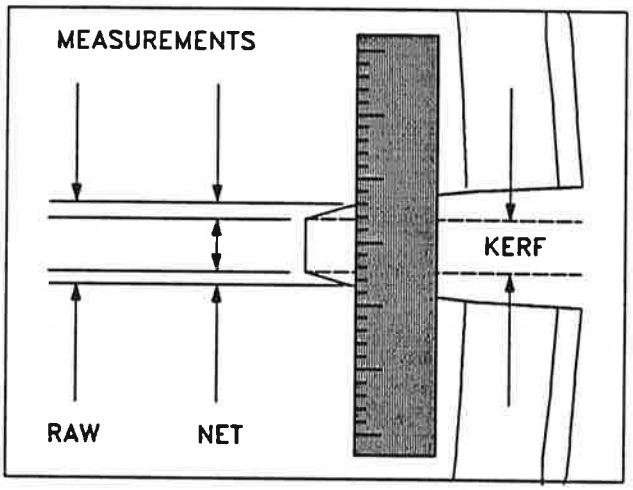

Figure 4. Manual Measurement of Saw Cut Profile.

2.2 Procedure Modifications

Although the AAR procedure is well suited for its original purpose, more detail is required if the reconstruction is meant to provide an accurate estimate of the residual stress distribution, rather than just a determination of wheel condition. Even the refined procedure is only a first step toward the more elaborate goal. Inspection of the published experimental results [3]

(a) half-symmetric (b) quarter-symmetric

Figure 5. Alternative Finite Element Models of Cut Wheel.

indicates measurement error on the order of 0.05 to 0.1 mm for the manual technique. There is also a tendency for the effects of displacements near the inner end of the cut to be amplified at locations far from the end. Thus, small errors near the inner end of the cut, incorporated into the profile of the finite element model, may cause larger errors in the computed outer rim hoop stress.

The experimental procedure for the first saw cut test of MU wheels was consequently modified to obtain more detailed information about rim stresses. In addition to the clip-gauge at the flange tip, the instrumentation included 2-gauge/90-degree strain rosettes at several locations on the tread and rim faces, and moire gratings approximately 50 mm wide were bonded to the flat areas of the rim faces [2].[8]

The primary instrumentation in these tests was the moire, which provided the cut profile displacement information. Figure 6 illustrates the measurement concept. A reference grating with a spacing $R = 1$ line/mm is shown in (a). Suppose a similar grating is bonded to a body which is then stretched laterally. If the reference and body gratings are superimposed, as in (b), the line density varies from 1/mm (fully lapped) to 2/mm (maximum separation), creating a pattern of light and dark fringes. The strain, S, can be determined from the distance between fringes, D, and the reference grating spacing:

$$S = \frac{1}{RD} \qquad (1)$$

8 The moire work, including design and fabrication of portable recording apparatus, was performed by Dr. R. Czarnek, at that time a member of the faculty of the Virginia Polytechnic Institute and State University, Blacksburg, VA. Shop support including the actual saw cutting was provided by the Norfolk Southern Railroad Research Laboratory, under the supervision of Mr. T.W. Ward.

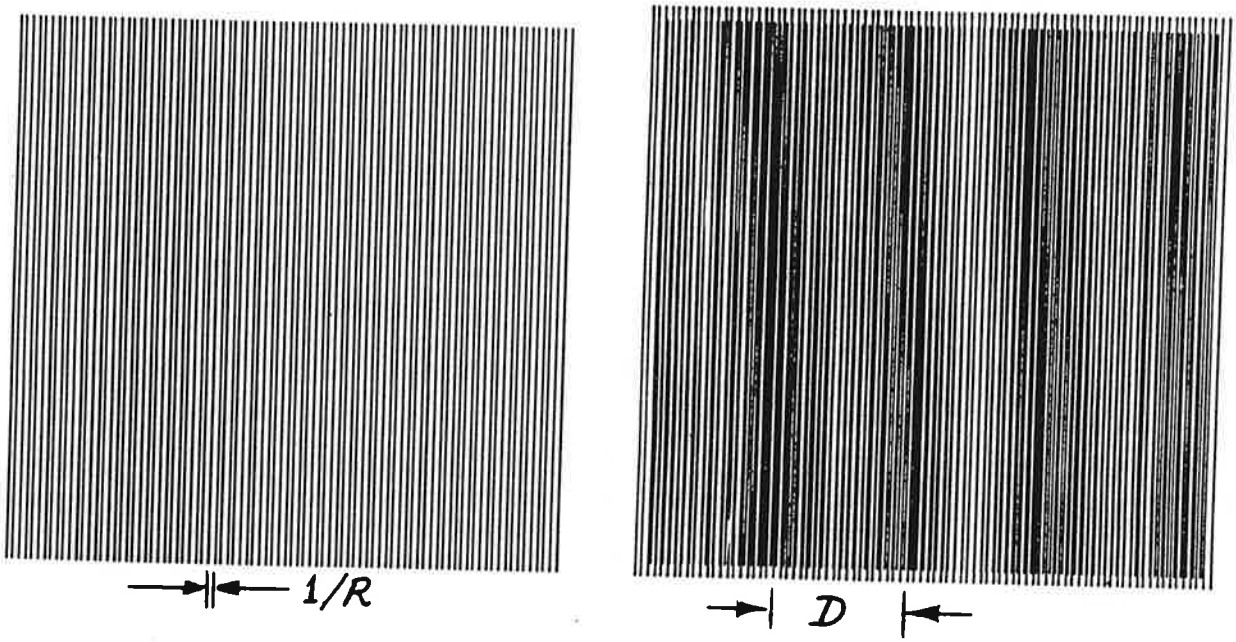

(a) reference grating

(b) fringe pattern

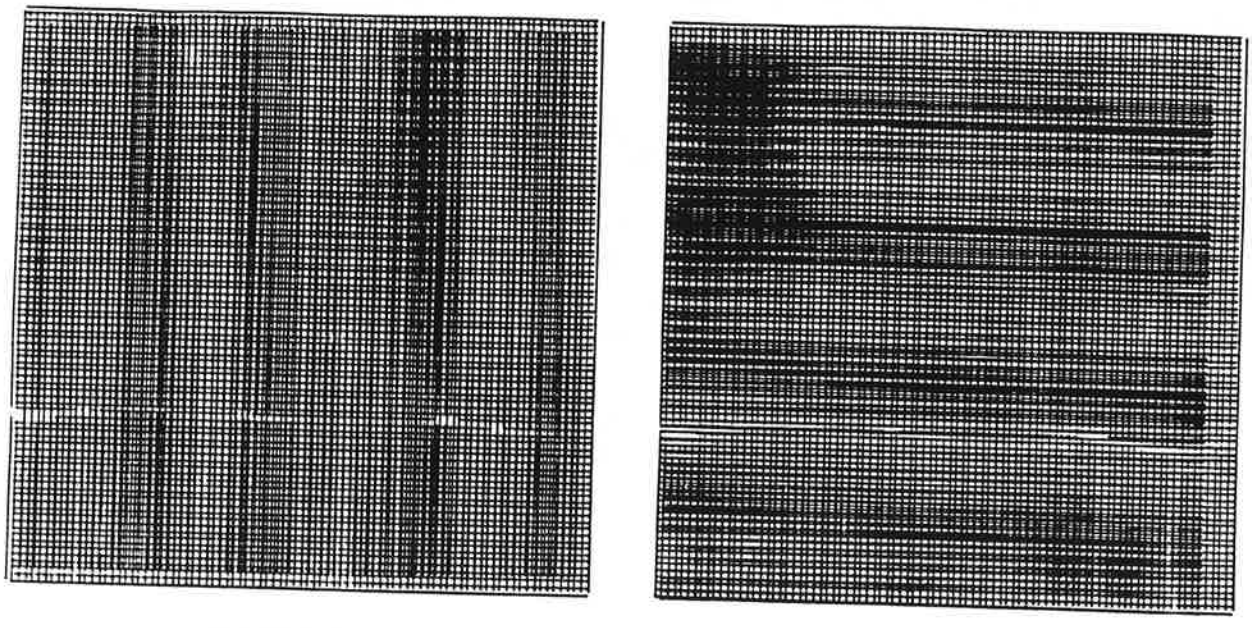

(c) X fringes

(d) Y fringes

Figure 6. Basic Principle of the Moire Method.

In a similar manner, the relative stretching displacement X between any two points on the body can be calculated from the number of fringes between the points, N, and the reference grating spacing:

$$X = \frac{N}{R} \tag{2}$$

If both lateral (X) and vertical (Y) displacements are sought, the body is instrumented with a cross-grating. The fringe patterns for each component are obtained individually by superimposing the reference grating first with vertical (c) and then with lateral (d) orientation.

In the actual wheel saw cut test, moire with spacing on the order of 1000 lines/mm. At such small spacings, the fringes are produced by diffraction, and laser illumination must be used to produce patterns sharp enough to allow measurement of the small displacements associated with stress relief. The measurement error is then reduced to the order of 0.01 mm. Cross-gratings provide the capability to measure radial as well as hoop displacement, but the radial displacement can only be measured relative to the tip of the cut. The cut must be stopped within the grating area to maintain continuity for proper counting of hoop displacement fringes across the opening (Figure 7). Also, the strain gauges must be located to one side of the grating, i.e., about 20 mm distant from the cutting line in the present case.

2.3 Test Results

One new wheel and one used wheel with center tread thermal cracks were tested [2]. The strain gauges were monitored, during cutting, in order to provide thermal strain data for evaluation of the effects of cutting heat. Each cut was stopped, within the rim, to allow for moire and strain gauge measurements, and was then continued into the plate and hub to obtain the complete clip-gauge curve. Two cuts located at opposite ends of a wheel diameter were made in each wheel (identified as #1 and #2 in the new wheel, and #3 and #4 in the used wheel).

The thermal effect of cutting was minimized by a combination of low saw speed, low blade travel rate, and continuous lubrication. Some degree of heating was unavoidable despite these precautions, however, and the effect was inferred from gauge strain-time histories. Each gauge on the rim faces exhibited a strain peak, as the tip of the cut passed the gauge location, consisting of thermal and release contributions. An upper bound on temperature at the gauge location was obtained by assuming the peak was caused solely by thermal expansion at the nominal rate of 6.5 microstrain/^{o}F (11.7/^{o}C). Maximum temperature rise at the gauge locations was thus estimated to be 170 ^{o}F (77 ^{o}C). Although the local temperature rise at the cut surface must have been considerably higher, it is unlikely to have reached the lower limit of the metallurgical phase transformation range, 1333 ^{o}F (723 ^{o}C).

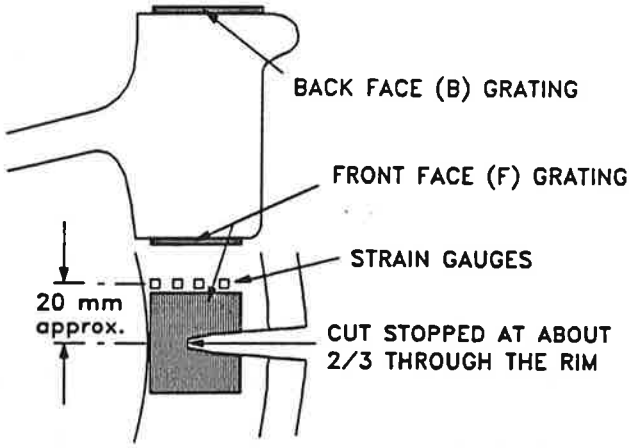

Figure 7. Cut Profile Measurement with Moire.

When the cut was stopped at about 2/3 through the rim, the clip-gauge was removed, and the wheel was allowed to cool to ambient temperature[9] before any further measurements were made. Strain release readings were then recorded from the strain gauges, the wheel was removed from the saw table, and holograms of the moire gratings were taken. After completion of these measurements, the wheel was returned to the saw table, the clip-gauge was re-applied, and the cut was continued. These steps were repeated for each cut. Thus, the data obtained from cut #2 were influenced to some degree by the presence of the full cut #1, and the data from cut #4 were similarly affected by cut #3.

The hoop strain release readings across the tread of the new wheel were nearly uniform, averaging about 1400 microstrain at cut #1 and 1350 microstrain at cut #2. The pre-cut hoop residual stress inferred from these values is 276 to 280 MPa (40 to 42 ksi) compression. The rim face gauges indicated a declining compression trend radially inward and reversal to tension at locations beyond the tip of the cut. The corresponding readings from the used wheel were distinctly nonuniform, of the order of 500 microstrain in magnitude or less, with little evidence of any trend. The pre-cut hoop stress inferred from averages of the tread strain gauge readings was about 24 MPa (3.5 ksi) compression at cut #3, but 32 MPa (4.6 ksi) tension at cut #4. The low values and sign change suggested that the used wheel had been stress relieved before the saw cut test. However, contradictory results indicating the presence of significant residual compression were obtained from the stress reconstruction analysis (see Section 3).

One direct comparison was made between strain gauge and moire strain release readings. In the case of cut #2, damage to the front face grating prevented the acquisition of hoop displacements across the cut. However, the fringes on the strain-gauged side were analyzed for hoop strains at several distances from the cut surface. These results were consistent with

---

9 This was verified by means of a magnetized bimetal thermometer of a type commonly used to measure rail temperature in the field.

the strain gauge readings (Figure 8). The large strain magnitudes indicated by moire close to the tip of the cut suggest that the cutting process itself caused considerable local plastic deformation.

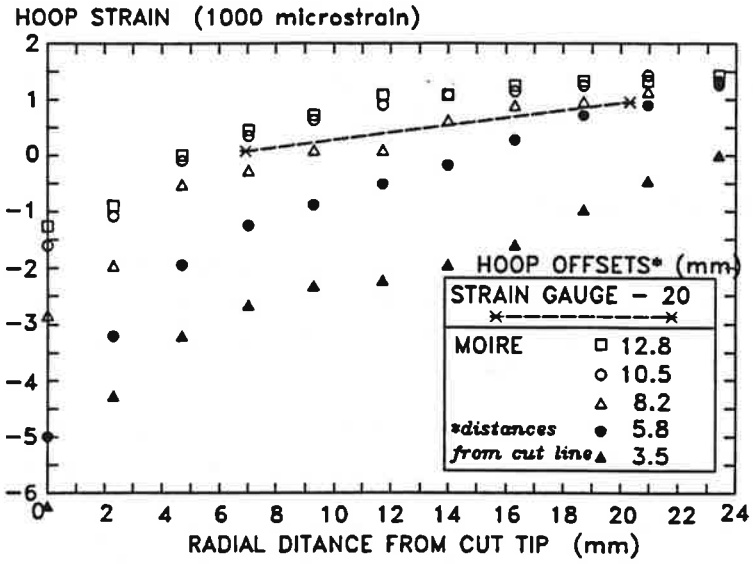

Figure 8. Hoop Strains Measured Near Cut #2.

The other gratings survived the test and provided usable displacement data. Hoop displacements across the cut and radial displacements relative to the tip of the cut were measured. Table 1 (page 15) summarizes the results for the new wheel, based on measurements at points 2.3 mm circumferentially from the cut surfaces. The location values in the left hand column are radial distances from the tip of the cut toward the flange. For the used wheel, some measurements were made at 4.7 mm as well as 2.3 mm from the cut surfaces, as indicated by the "distance" values in the upper margins of Tables 2 and 3 (page 16).

Figure 9 compares the hoop displacement profiles obtained from the two wheels. The results are theoretically self-corrected for the kerf, but some measurement error is evident in the deviations from zero displacement at the tip of the cut. The profile curves appear to be repeatable on each face for each wheel, the differences being within the margin of error implied by the deviations at the cut tip. The most striking result is the retention of a definite closure tendency in the used wheel, even though the magnitude is only 10 to 20 % of the closure exhibited by the new wheel.

3. RECONSTRUCTION ANALYSIS PROCEDURE AND RESULTS

The repeatability of both strain gauge and moire results suggested that the first cut in each wheel had little effect on the release characteristics of the second cut, at least so far as the behavior up to 2/3 through the rim. Therefore, the reconstruction analysis procedure was simplified in two ways. First, the cut profile data was averaged in those cases where two or more sets of measurements were available (1B and 2B, 3F and 4F, 3B and 4B), and the hoop displacement curves were faired to zero at the cut tip. Second, the quarter-symmetric modeling approach was adopted, Figure 5(b).[10]

3.1 Finite Element Models and Procedure

Separate models were prepared for the new and used wheels in order to match their rim thicknesses (Figure 10). These grids were adapted from an earlier version of the heat transfer finite element model discussed in the third report in this series. The NIKE3D finite element software [16] was used for the analyses.

The averaged and faired profile displacements were linearly interpolated to provide equivalent values at each model node point on the cut surface. The profile curves were also extrapolated to provide values at the nodes beyond the moire, i.e., along the rim front face bevel, tread, and flange. The nodal displacement values[11] were added to the nominal profile section coordinates to define the initial geometry of the model on the cutting plane.

Displacements of equal magnitude but opposite sense were applied as boundary conditions to close the cut, and the elastic stresses corresponding to these displacements were computed. The stresses computed in this way are of the same sense as the relieved stresses.

3.2 Analysis Results

Reconstruction analyses were performed with and without the radial displacement information. Comparison of the results revealed the significance of the radial displacements.

The accepted procedure heretofore has been to neglect the radial displacements because they are difficult to measure. This simplifying assumption was based on estimates, made during the freight car wheel survey mentioned earlier, which indicated that the radial displacement magnitude should not exceed 10% of the hoop displacement magnitude.

---

10 Strictly speaking, quarter-symmetric reconstruction should be applied to an experiment in which release measurements are made only after two identical cuts have been made at the opposite ends of a diameter. Application to the present results is justified only by the apparently small influence of the cuts on each other.

11 Half the hoop displacement values to properly reflect the model symmetry.

Table 1. Moire Displacement Measurements (New Wheel).

Cut no.	1				2	
Face	Front rim face		Back rim face		Back rim face	
Component Loc. (mm)	Hoop (μm)	Radial (μm)	Hoop (μm)	Radial (μm)	Hoop (μm)	Radial (μm)
0.0	- 31.0	8.0	- 45.0	14.0	- 12.5	6.9
2.3	- 77.0	14.0	- 66.0	13.0	- 36.7	9.8
4.7	- 119.0	16.0	- 89.0	10.0	- 65.9	9.0
7.0	- 151.0	18.0	- 112.0	8.0	- 90.9	9.2
9.3	- 183.0	20.0	- 135.0	6.0	- 115.9	8.5
11.7	- 212.0	21.0	- 156.0	5.0	- 137.6	9.4
14.0	- 239.0	22.0	- 178.0	4.0	- 161.0	10.0
16.3	- 267.0	24.0	- 199.0	2.0	- 183.9	10.6
18.7	- 294.0	24.0	- 221.0	1.0	- 207.7	11.3
21.0	- 318.0	23.0	- 243.0	0.0	- 229.4	11.5
23.4	- 342.0	23.0	- 264.0	- 1.0	- 251.0	12.3
25.7	- 365.0	22.0	- 286.0	- 2.0	- 274.4	12.7
28.0	- 387.0	22.0	- 306.0	- 3.0	- 296.5	13.1
30.4	- 408.0	21.0	- 326.0	- 5.0	- 319.8	13.8
32.7			- 348.0	- 5.0	- 341.5	14.0
35.0			- 367.0	- 7.0	- 362.8	14.4
37.4			- 386.0	- 9.0	- 384.9	14.4
39.7			- 404.0	- 11.0	- 404.5	13.1
42.0			- 422.0	- 12.0	- 424.5	11.5
44.4			- 440.0	- 14.0	- 444.1	10.0
46.7			- 457.0	- 16.0	- 463.3	8.5
49.0			- 474.0	- 19.0	- 482.9	7.1
51.4			- 490.0	- 21.0	- 503.3	6.3
53.7			- 507.0	- 23.0	- 521.7	4.6
56.1			- 523.0	- 25.0	- 538.8	2.9
58.4			- 538.0	- 28.0	- 555.0	0.4
60.7			- 554.0	- 30.0	- 571.3	
63.1			- 569.0			

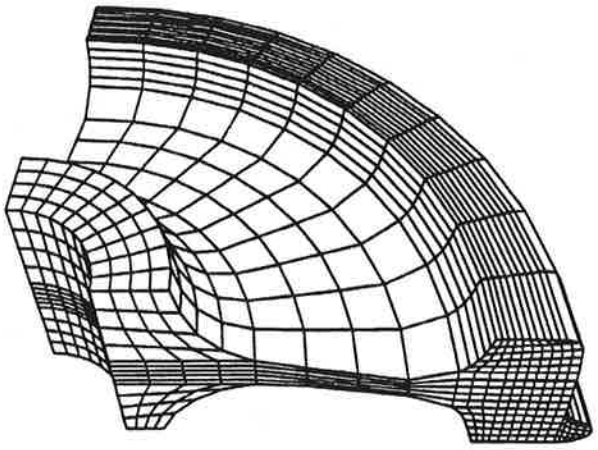

(a) new wheel

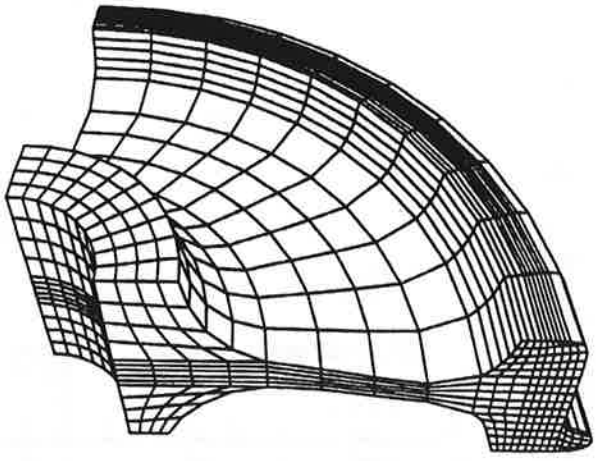

(b) used wheel

Figure 10. Quarter-Symmetric Finite Element Models.

The moire data in Tables 1 - 3 confirm the assumption. The radial displacements for the most part do not exceed 5% of the hoop displacements, except where both components are quite small and at a few locations on the used wheel.

A different picture emerged, however, from comparative reconstruction analyses of the new wheel. The hoop stress magnitude was found to be 27% greater, when the radial displacements were included in the model, than the magnitude obtained by considering the hoop displacements alone. Therefore, all reconstructed stresses presented in the rest of this report include the radial displacement effect.

Figure 11 illustrates the contours of reconstructed hoop stress computed for the new and used wheels. Both cases exhibit significant lateral variation, a result not unexpected when the differences between the front and back face cut profiles (Figure 9) are considered. Both cases also exhibit an apparent reversal from compression to tension, deeper in the rim, where the tip of the cut is approached. A similar effect was observed in the rim face strain gauge results (Section 2.3). However, the extent of the apparent tensile zone is a surprising result for the new wheel, and some questions must therefore be raised about the interpretation of reconstructed stresses (see Section 4).

The most useful figure of merit for comparison of the two cases is an average stress, in the center tread region, at about the depth below tread expected for typical thermal cracks. This is represented by a value between contours A and B for the new wheel, or about 290 MPa (42 ksi) compression. Applying the same rule of thumb to the used wheel suggests a value between contours B and C, or about 140 MPa (20 ksi) compression. Although this is more than a factor of two reduction, the reconstructed stress contradicts the estimate of total relief, before cutting, obtained from the tread strain gauge measurements (Section 2.3).

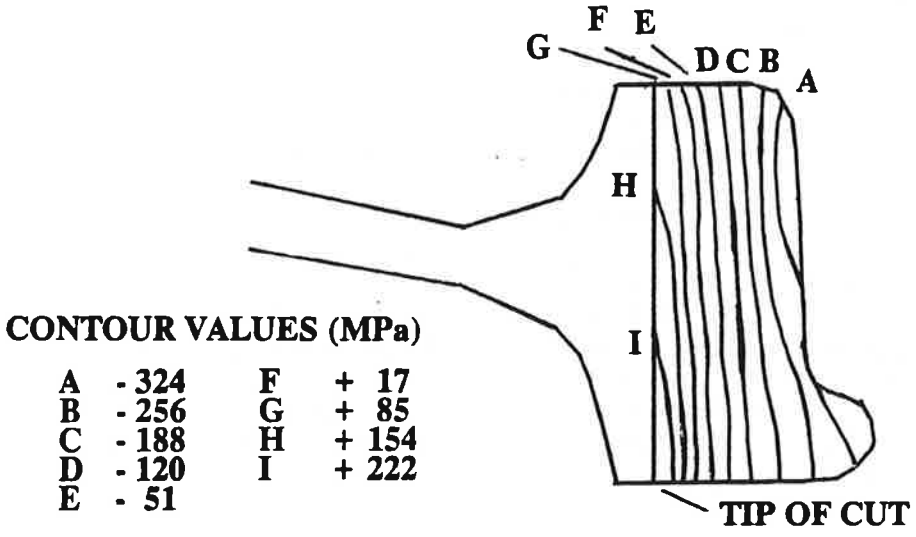

(a) new wheel

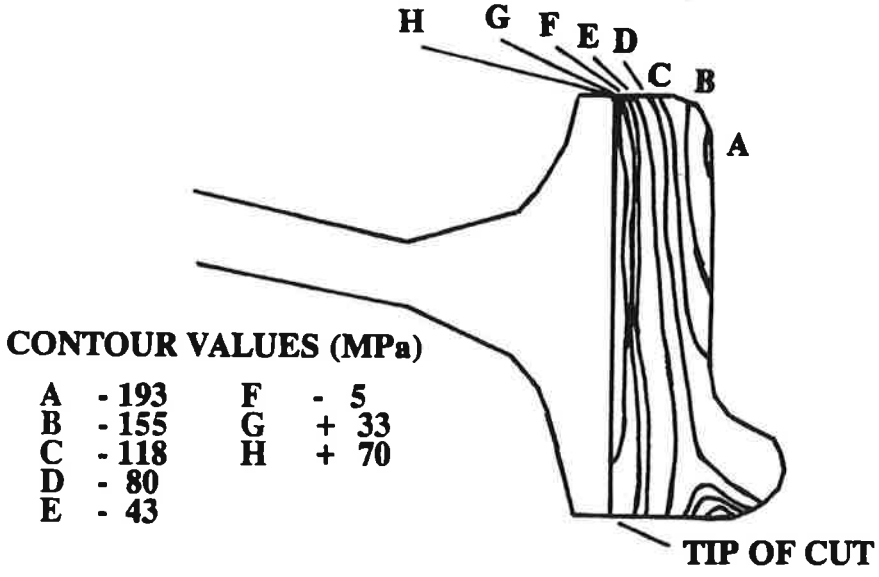

(b) used wheel

Figure 11. Contours of Reconstructed Hoop Stress (MPa).
(Positive - tension; negative - compression; 1 MPa ≅ 145 psi.)

4. PROCEDURE EVALUATION

The significant change of reconstructed hoop stress, observed when account was taken of radial displacements, suggested the need for further evaluation of the saw cutting test. The information being acquired is still quite limited, even with moire instrumentation. The following kinds of measurements have not yet been made: (1) distribution of cut profile displacements across the tread and flange; (2) absolute radial displacement (i.e., referenced to the wheel rotation axis); (3) lateral (back-to-front) displacements; (4) displacements on the cut surfaces; (5) distribution of displacements along the extended cutting line (i.e., radially inward beyond the tip of the cut); and (6) distributions, on the front and back faces, over areas surrounding the cut as well as the extended cutting line. Some of these measurements are probably not technically feasible, others may be feasible but expensive, and a few might be practical after further development of the test procedure.

Therefore, it is certainly worthwhile to consider how well the present procedure approximates the actual stress relief, and what benefits can be gained by adding other practical measurements. A numerical simulation was devised and has been used to find a preliminary answer to the first question.

4.1 Numerical Simulation Procedure

The numerical simulation is based on a common characteristic of residual and thermal stresses. Both types are self-equilibrating and, therefore, simulated residual stresses can be generated by computing the thermal stresses in a body subjected to nonuniform temperature but otherwise unrestrained and unloaded. Although the stresses computed in this way cannot be associated with any specific physical process that leaves residual stresses in a wheel at ambient temperature, they can still provide exact values for the stresses released by a hypothetical saw cutting test.

The simulation was conducted by using the TOPAZ2D computer program to establish axisymmetric but radially and laterally nonuniform temperature distributions in the new wheel model. Transient heating and elastic thermal stress analyses were conducted, using the heat flux profile shown in Figure 12. Since the analyses did not involve any dynamic effects, the transient stress distribution at a convenient time could be treated as a residual stress distribution.

Two cases were created by extracting the temperature distributions at the two times indicated in the figure. The first case produced a steep temperature gradient and a concentration of thermal stress in the outer rim region. The second case produced an average rim temperature much higher than that in the plate and a low-gradient distribution of thermal stress throughout the rim. These cases were selected to bracket the probable characteristics of the actual residual stress distribution in a new wheel.

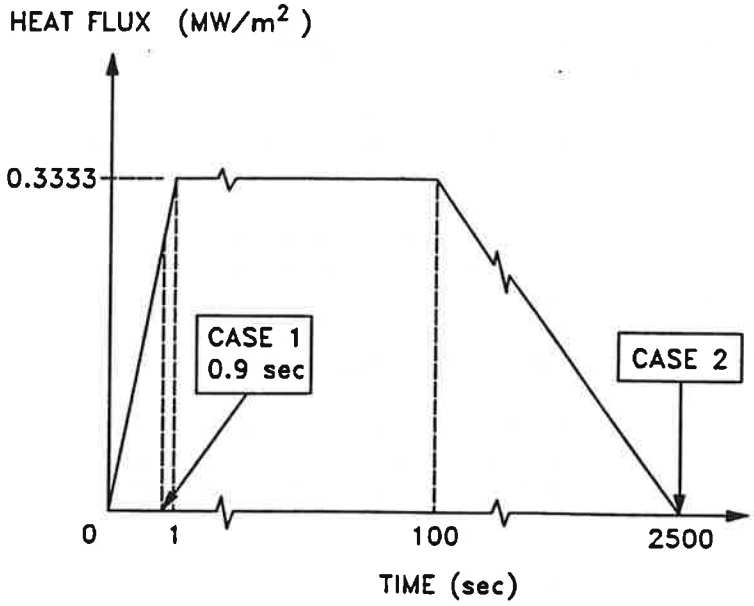

Figure 12. Heat Flux Versus Time for Residual Stress Simulations.

In each case, the computed temperatures were applied to all radial sections of the corresponding quarter-symmetric finite element model; see Figures 5(b) and 10(a). This model possessed the initial geometry of the undeformed wheel, i.e., the cut coincided with the cutting line symmetry plane. An elastic analysis was then performed with the NIKE3D computer program, and the results of that analysis were used to construct the simulation in two steps, as follows.

First, stresses were computed on the quarter-symmetry and cutting line planes, indicated by the hatched boundaries in Figure 5(b). The stresses on the quarter-symmetry plane were assumed to be the values of the simulated residual stresses in the uncut body. The stresses on the cutting line plane represent the simulated residual stresses after cutting. Therefore, the differences between these two sets of data were taken, point by point in the section profile, to represent the exact values of the stresses released by cutting.

Second, the hoop and net[12] radial displacements were computed at each nodal point, along the cut, on the flat surfaces of the front and back faces. The net radial displacments were then modified to relative values by subtracting the value computed for the tip of the cut.

---

12 The gross radial displacement includes a contribution from thermal expansion. The net value, i.e. that portion due to the cut, is the difference between the gross values at similar nodes on the cutting line and quarter-symmetry planes.

The modified displacements were treated as the results of hypothetical saw-cutting tests, like that described in Section 2.2, but with no measurement error. The modified displacements were interpolated and extrapolated, to cover the cut surface, and were applied to a quarter-symmetric model, as described in Section 3.1, to perform the reconstruction analyses.

Similar reconstruction analyses were also performed with the hoop and unmodified net radial displacements specified at every node on the cut surface. These analyses simulated the results of hypothetical idealized tests with instrumentation capable of error-free measurement of hoop and absolute radial displacements on the entire cut surface.

4.2 Simulation Results

Figures 13 and 14 illustrate the results for the simulation of the practical experiment. Contours of released hoop stress are shown: the exact values in part (a) and the reconstructed results in part (b) of each figure. The reconstructed results evidently bear little resemblance to the exact values. The reconstructed magnitudes are low by a factor of 5 to 10, and the contour patterns are not properly reproduced.

Figures 15 and 16 are similar illustrations for the simulation of the idealized experiment. In these cases, the reconstructed results are in generally good agreement with the exact values, although the contours in the flange area are not well reproduced in the second (low gradient) case.

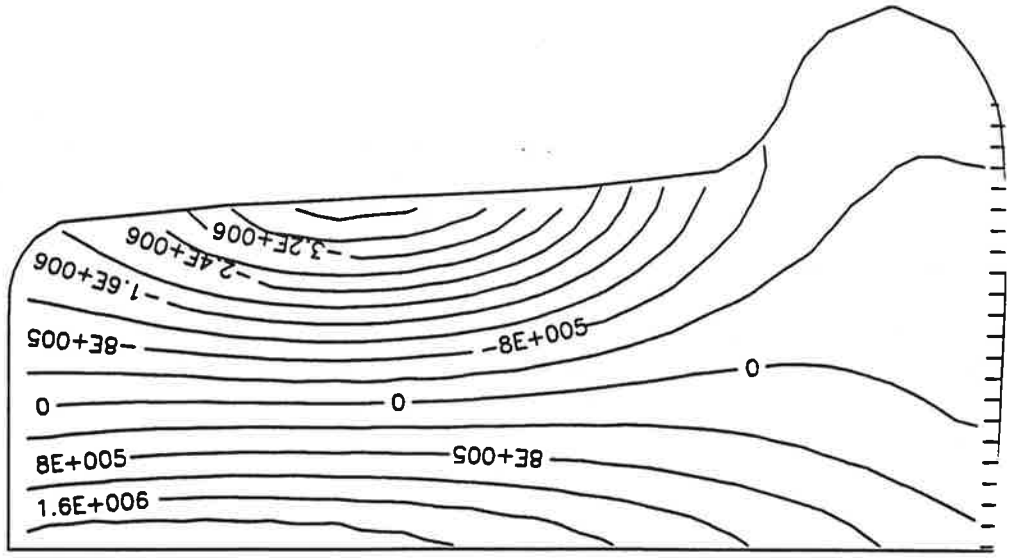

(a) exact values

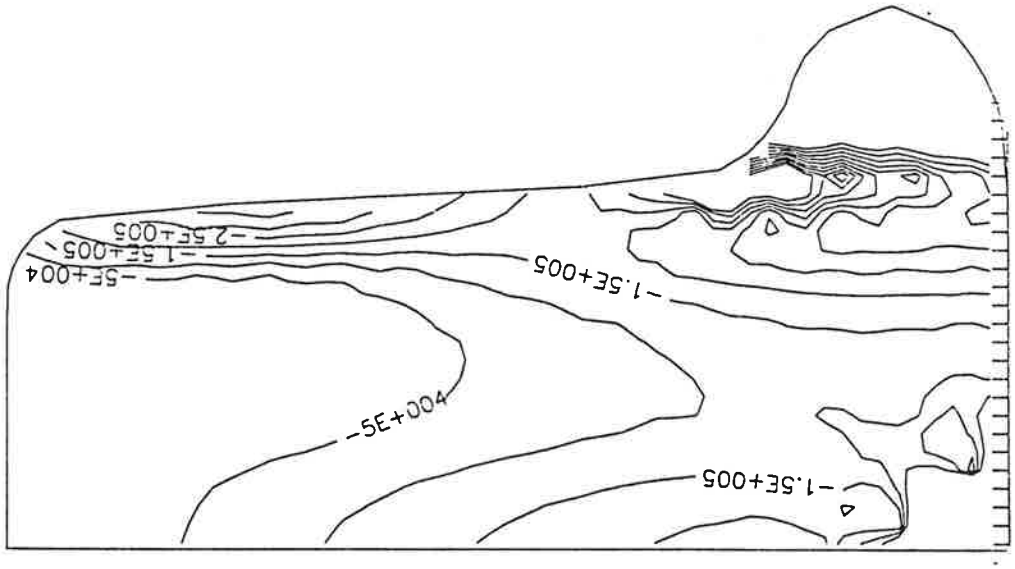

(b) reconstructed values

Figure 13. Contours of Released Hoop Stress from Simulation Case #1. (Arbitrary units.)

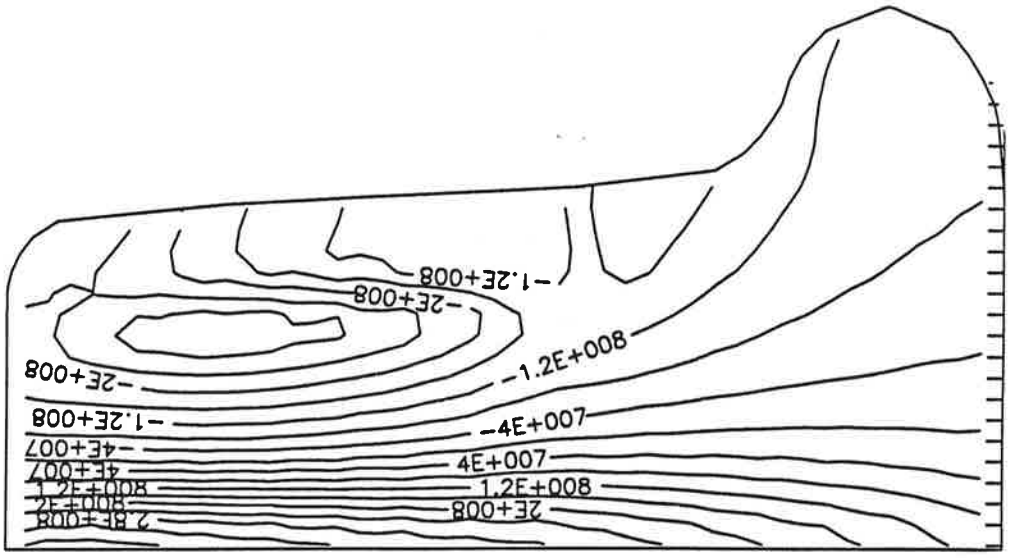

(a) exact values

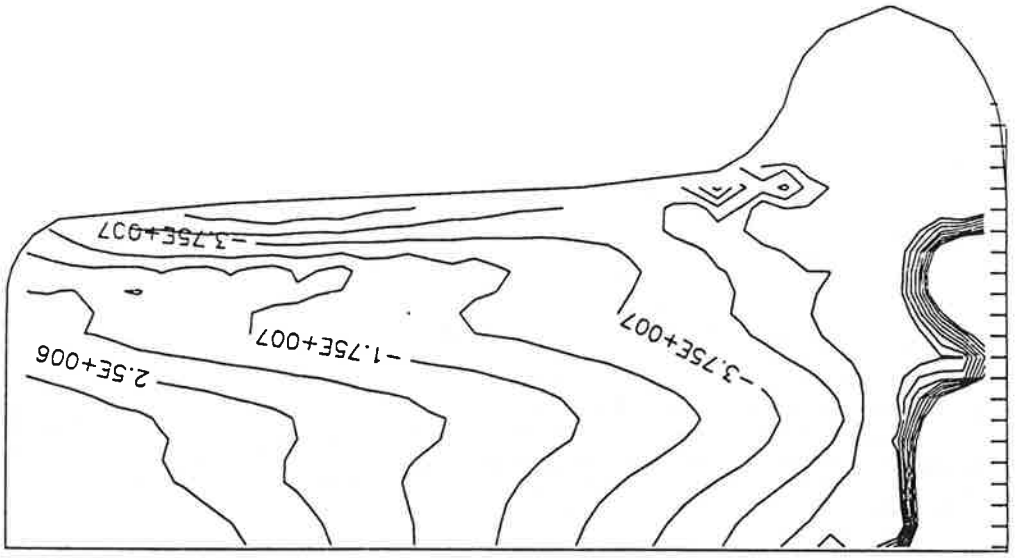

(b) reconstructed values

Figure 14. Contours of Released Hoop Stress from Simulation Case #2. (Arbitrary units.)

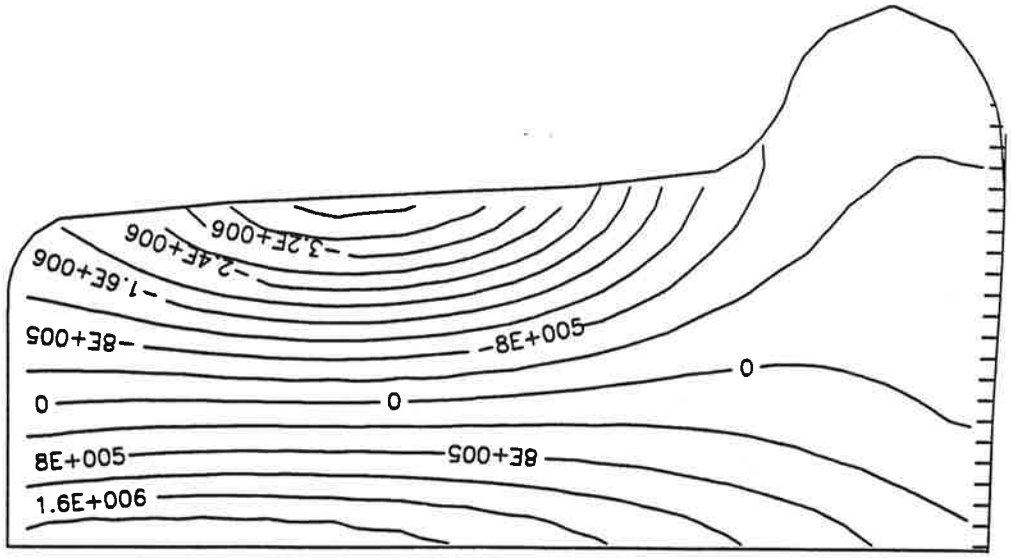

(a) exact values

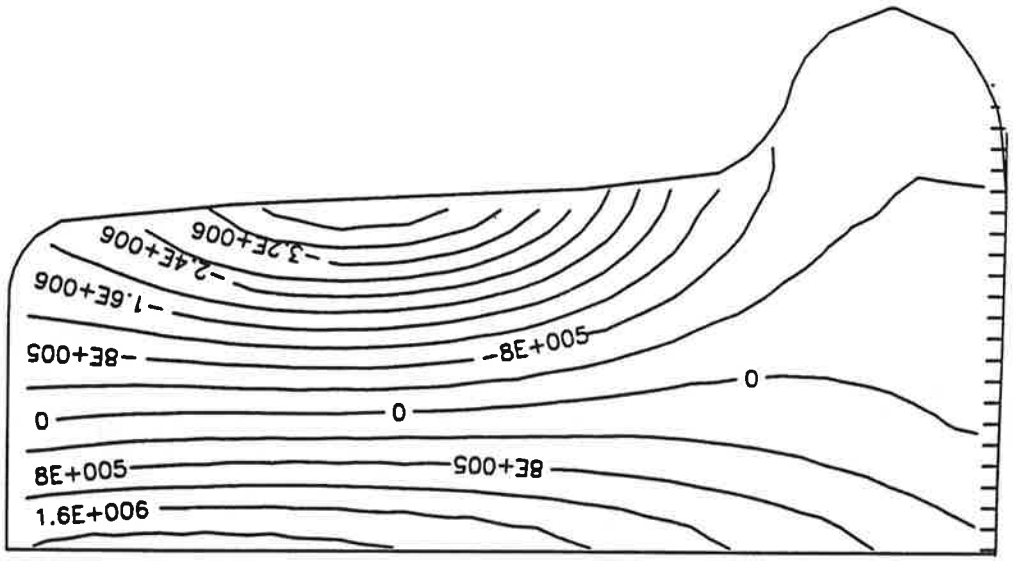

(b) reconstructed values

Figure 15. Contours of Released Hoop Stress from Idealized Case #1. (Arbitrary units.)

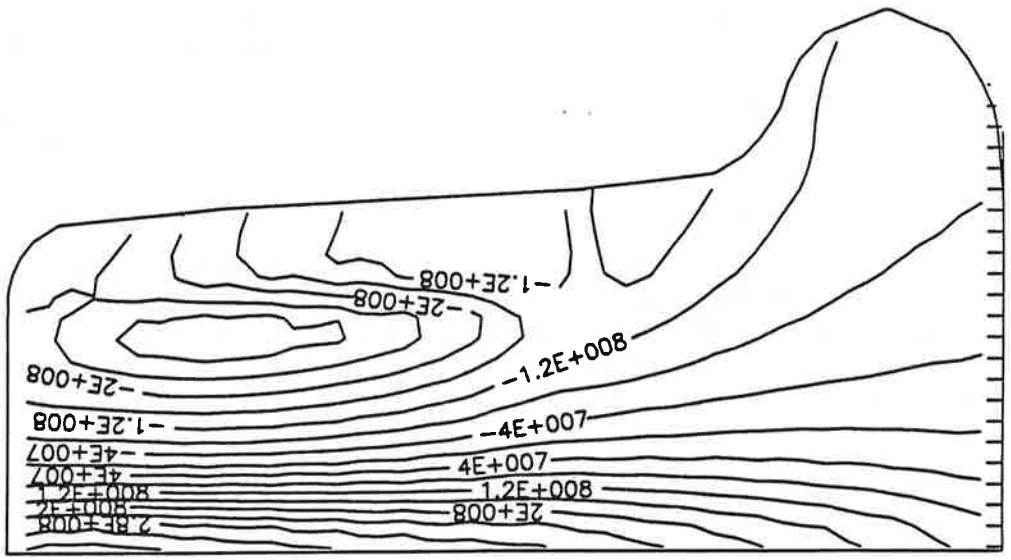

(a) exact values

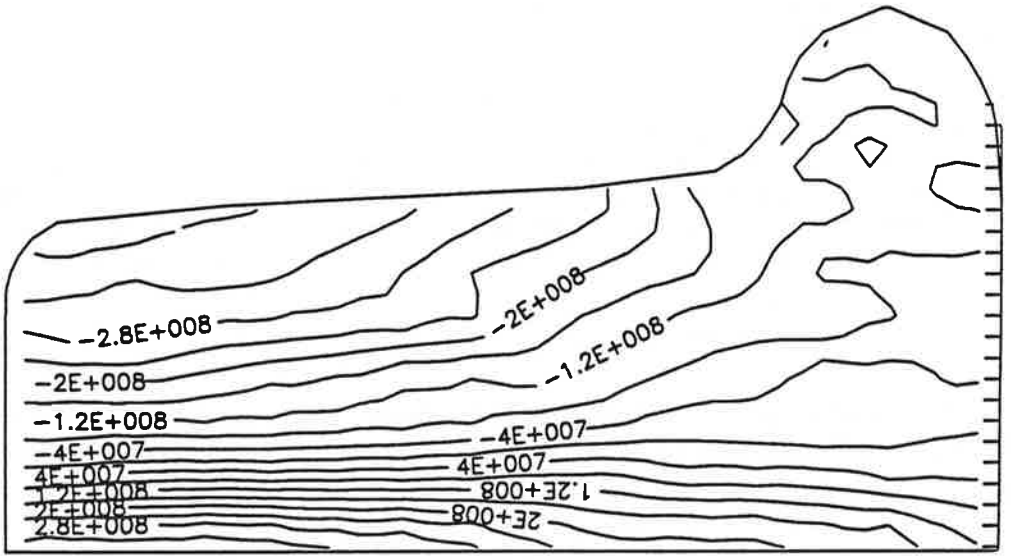

(b) reconstructed values

Figure 16. Contours of Released Hoop Stress from Idealized Case #2. (Arbitrary units.)

[10] A.B. Perlman, J.E. Gordon, and O. Orringer, "Effect of grinding strategy on residual stress in the rail head," *Proc. FRA/ERRI International Conference on Rail Quality and Maintenance for Modern Railway Operation*, Delft, The Netherlands, June 1992 (in press).

[11] K.L. Johnson, *Contact Mechanics*, Cambridge University Press, Cambridge, England, 1985.

[12] A. Martin Meizoso, J.M. Martinez Esnaola, and M. Fuentes Pèrez, "Approximate crack growth estimate of railway wheel influenced by normal and shear action," *Theoretical and Applied Fracture Mechanics 15*, 179-190 (1991).

[13] R. Lundèn, "Contact region fatigue of railway wheels under combined mechanical rolling pressure and thermal brake loading," *Wear 144*, 57-70 (1991).

[14] S.M. Patil and B.R. Rajkumar, "An analytical method for determining residual stresses in railroad wheels," *Proc. IEEE-ASME Joint Railroad Conference*, Toronto, 1987.

[15] D.H. Stone, B.R. Rajkumar, and W.J. Harris, Jr., "Wheel thermal failure mechanisms in heavy haul operations," *Proc. 9th International Wheelset Congress*, Montreal, 1988.

[16] B.N. Maker, R.M. Ferencz, and J.O. Hallquist, "NIKE3D - A nonlinear, implicit, three-dimensional finite element code for solid and structural mechanics," Lawrence Livermore National Laboratory, Livermore, CA, UCRL-MA-105268, January 1991.

[17] A.B. Shapiro, "TOPAZ2D - A two-dimensional finite element code for heat transfer analysis, electrostatics, and magnetostatics problems," Lawrence Livermore National Laboratory, Livermore, CA, UCID-20824, July 1986.